

Supporting Information

**Harvesting temperature fluctuations as electrical
energy using torsional and tensile polymer muscles**

Shi Hyeong Kim^a, Márcio D. Lima^b, Mikhail E. Kozlov^b, Carter S. Haines^b,
Geoffrey M. Spinks^c, Shazed Aziz^c, Changsoon Choi^a, Hyeon Jun Sim^a, Xuemin Wang^d,
Hongbing Lu^d, Dong Qian^d, John D. W. Madden^e, Ray H. Baughman^{*b} & Seon Jeong Kim^{*a}

^aCenter for Bio-Artificial Muscle and Department of Biomedical Engineering, Hanyang University, Seoul 133-791, South Korea. [*] E-mail: sjk@hanyang.ac.kr

^bAlan G. MacDiarmid NanoTech Institute, University of Texas at Dallas, Richardson, TX 75083, USA. [*] E-mail: ray.baughman@utdallas.edu.

^cIntelligent Polymer Research Institute, ARC Centre of Excellence for Electromaterials Science, University of Wollongong, Wollongong, New South Wales 2522, Australia.

^dDepartment of Mechanical Engineering, University of Texas at Dallas, Richardson, TX 75080, USA.

^eDepartment of Electrical and Computer Engineering and Advanced Material and Process Engineering Laboratory, University of British Columbia, Vancouver, British Columbia V6T 1Z4, Canada.

Corresponding author emails: sjk@hanyang.ac.kr; ray.baughman@utdallas.edu.

MATERIALS AND METHODS

1. Muscle preparation

The precursor monofilament nylon 66 fibers deployed for fabrication of torsional muscles were obtained from the following commercial sewing threads: Coats & Clark D64 (27- μm -diameter monofilaments fibers were extracted from this multifilament thread), The Thread Exchange, Inc. monofilament MON003CLR01S (76 μm diameter), Coats & Clark D67 4 mil (102 μm diameter), and Coats & Clark D67 5 mil (127 μm diameter). Additionally, nylon 6 fibers used for fishing lines (400, 500, 780, and 1000- μm -diameter Sport Fisher monofilament) were deployed as precursors for torsional muscles. Twist insertion was accomplished by attaching one end of the precursor nylon fiber to the shaft of a stepper motor. The other end of the polymer was attached to a weight, which was prevented from rotating. The applied weight determined the spring index and bias angle of coiled fibers (which decreased and increased, respectively, with applied load), and was sufficiently high that it prevented fiber snarling during twist insertion. The turns/meter of inserted twist was calculated by dividing the inserted turns by the final muscle length. Using the fiber bias angle observed on the fiber surface by optical microscopy, the turns/meter was also calculated using $\text{turns/m} = \tan^{-1}(\pi\tau D)$, where D is the fiber diameter and τ is the amount of twist inserted per initial fiber length.

Twisted nylon 6,6 fiber muscles were prepared by twisting a highly oriented precursor fiber under 26 MPa tension until just below the onset of coiling, which provided a polymer chain bias angle with respect to the fiber direction of about 45° on the fiber surface. Coiled fibers were made by further inserting twist until complete coiling occurred. Following twist insertion, the fiber was subjected to heat treatment under vacuum at 210°C for 2 hours, while constant length was maintained. This length corresponded to that of the non-strained muscle at room temperature before annealing. Here and elsewhere, unless otherwise noted, tensile stresses are normalized with respect to the cross-sectional area of the fiber before twist insertion. Muscle fibers that are twisted below the twist level required for coiling are called “twisted fibers” or “twisted muscles” and those that are twisted to provide coiling are called “coiled fibers” or “coiled muscles”. Unless otherwise indicated, the term “fiber diameter” for a muscle (whether twisted or coiled) refers to the diameter of the precursor non-twisted fiber used to make the muscle.

As an example, twisted muscle fiber was prepared by inserting 8,350 turns/m of twist into a 27- μm -diameter nylon 6,6 fiber that supported a constant mass (corresponding to 26 MPa initial stress). The twisted fiber diameter was 29 μm and its bias angle was 45°. Coiled muscle fiber was prepared by inserting an additional 2,850 turns/m of twist into the above twisted fiber, without changing the applied tensile load. The outer diameter of the non-loaded coil was 62 μm and its spring index was 1.14. The ratio of fiber volume to coil volume (including void volume) in a coiled muscle was 1.52.

SZ fiber was prepared by essentially the same process as for twisted or coiled Z (or S) muscle fibers, except that separate steps were used for making the S and the Z muscle segments. In the first step, twist was inserted in the top-half of the fiber by attaching a weight at the fiber centre and prohibiting this centre from rotating, while the top of the fiber was twisted using a rotary motor. In the second step, the upper and lowered fiber ends were exchanged, and the above twist insertion process was repeated, but by inserting twist in the opposite rotational direction.

Twisted 27, 76, 102 and 127- μm -diameter fibers were obtained by inserting 8,350; 3,240; 2,570; and 2,220 turns/m of twist, respectively, under 26 MPa load. Coiled 27, 76, 102 and 127- μm -diameter fibers were obtained by inserting 11,200; 4,980; 3,700; and 3,250 turns/m of twist, respectively, under this same 26 MPa load. The resulting coiled fibers of 27,

76, 102 and 127- μm -diameter precursor fibers provided similar ratios of the initial fiber precursor length to the final non-loaded fiber length (4.5, 4.02, 4.05 and 4.0, respectively).

For conversion of thermal energy to electrical energy using tensile contraction, the muscle fibers were made from high-molecular-weight, 2-mm-diameter, braided polyethylene fibers that are sold as 35-pound-test PowerPro[®] fishing line (which were dyed green to minimize detectability by fish). Individual coiled muscle fibers were made by inserting twist into four of these parallel fibers under 10 MPa load until complete coiling resulted. The coiled fiber was not annealed. For electrical energy harvesting, using alternating hot and cold water, four of these muscles were operated in parallel inside a 9-mm-inner-diameter, 12-mm-outer-diameter silicone tube that was used to alternatively transport hot and cold water.

2. Characterization methods for tensile and torsional actuation and conversion of torsional mechanical energy to electrical energy

The setup shown in Fig. S1 and Video S3 was used for characterizing torsional rotation speed and torsional stroke. A magnetic rotor was attached at the midpoint of a torsional muscle, and the end of the magnet was maintained at a minimum separation during rotation of about 1.3 mm from an induction coil. The induction coil, which was extracted from a watch (Morioka Tokei Inc., Y481C movement), comprised an iron core wound with an insulated 20- μm -diameter wire. The coil resistance was 3.2 k Ω and the length and diameter of the coil were 8.5 mm and 2.3 mm, respectively. The voltage output from this induction coil was connected to an oscilloscope using a 10 M Ω impedance probe. The number of peaks in the voltage versus time signal provides the number of muscle rotations (and thereby the rotation angle) and the temporal separation between voltage peaks yields the torsional rotation speed. For comparative studies of torsional actuation for one-half-heated and fully-heated harvesters using twisted and coiled muscles made from 27- μm -diameter precursor fibers (Fig. 2(a) and Fig. S2), the magnetic rotor comprised two axially magnetized NdFeB-N50 cylindrical magnets from Excelpoint Corporation, each of which has a diameter of 1 mm, a thickness of 0.5 mm, and a mass of 2.85 mg. Their N50 indicates the maximum energy product in Mega-Gauss Oersteds (MGOe). These magnets were attached at the midpoint of the muscle array using inter-magnet attraction, so that the axial magnetization direction was orthogonal to the muscle fiber. In order to increase the moment of inertia of the magnetic rotor for other experiments (Fig. 2(b)), the number of connected magnets was increased to up to five pairs, which provided moments of inertia of 8.97×10^{-13} , 4.77×10^{-12} , 1.45×10^{-11} , 3.29×10^{-11} , and 6.28×10^{-11} kg $\cdot\text{m}^2$, respectively, as the number of magnet pairs increased from 1 to 5.

A different coil structure was needed to maximize average electrical power output for much larger fiber diameter muscles (like the coiled 102- μm -diameter nylon 6,6 fiber of Fig. 4), since the iron core of the watch-derived mechanical energy harvester interacted with the magnetic rotor to disturb torsional oscillations when we scaled rotor size with fiber size. To eliminate this problem for the coiled 102- μm -diameter nylon 6,6 fiber used for the energy harvesting experiments of Fig. 4, we used this coiled SZ fiber to torsionally rotate the axis of a hollow cylindrical neodymium magnet within a set of three coils. Both the magnet and coils were from a vibration micro-motor (model CMS-V0716 from Hyundai Autonet Company). At the centre of the length of this coiled SZ muscle, the S coiled and Z coiled muscles were attached at opposite ends of the rotor of the magnetic generator using epoxy glue (Devcon 5 Minute Epoxy Gel). The hollow cylindrical neodymium magnet weighed 1.02 g, was 9.5 mm high in the axial direction, and had a 2.2 mm inner diameter and 4.6 mm outer diameter.

3. Supplementary experimental results on torsional actuation and electrical energy harvesting

3.1. Torsional actuation of SZ and ZZ fiber

In order to obtain performance comparisons, torsional muscles were prepared in SZ and ZZ configurations. The fiber diameter of the precursor nylon 6,6 was 27 μm and the upper and lower fiber segments were 37.5 mm long, after fiber stretching to provide isometric or isobaric load conditions. The extreme fiber ends were torsionally tethered (and additionally positionally tethered for isometric characterizations). Fiber loads for isobaric measurements and fiber strain for isometric measurements were selected (see corresponding strains and loads, normalized to the precursor fiber diameter, in the figure insets) to maximize the torsional speed of the magnetic rotor, which was a pair of cylindrical NdFeB-N50 magnets (1 mm in total length and 1 mm in diameter, having an 8.97×10^{-13} $\text{kg} \cdot \text{m}^2$ moment of inertia) that were attached at fiber midpoint (Fig. S1) by magnetic attraction. Unless otherwise indicated, all results in this section are for these muscles and for this magnetic rotor.

The SZ fibers can be driven by heating (with a hot air pulse) either one segment or both segments, while the ZZ fiber must be half-heated to provide useful results when torsionally tethered at extreme ends. The Fig. S2(a) results show that for each temperature change (ΔT) a fully-heated coiled SZ fiber provides much higher peak torsional speed and maximum rotation angle per total muscle length than the one-half-heated coiled ZZ fiber, and that for both fibers the peak torsional speed increases approximately linearly with temperature change. In all cases, for these and other fibers, the peak torsional speed occurs during retwist after untwist of the actuated segment, and the maximum rotation angle occurs during the initial untwist of the actuated segment.

The results of Fig. S2 (b-d) show that for each temperature change a twisted SZ or ZZ fiber provides a higher peak torsional speed than a similarly actuated (half-heated or fully-heated) coiled SZ or ZZ fiber. However, we selected coiled muscles for torsional energy harvesting, since the high torques needed for rapid magnet acceleration degraded the reversibility of torsional actuation of twisted muscles for ΔT above $\sim 45^\circ\text{C}$, while high reversibility was obtained for a ΔT of 65°C for the coiled muscles. Coiled, fully-heated SZ fibers were selected for torsional energy harvesting, since theoretical considerations and experiments show that a fully-heated muscle fiber is more effective in converting the thermal energy of a temperature change to rotor kinetic energy than is a half-heated, coiled SZ or ZZ fiber (see Fig. 2(a) and Fig. S2(a)). Isometric torsional actuation was chosen for torsional energy harvesting both because of convenience of deployment and because the experimental results of Fig. S2 (b) show that optimized isometric actuation provides a slightly higher peak rotor speed (and therefore higher rotor kinetic energy for electrical energy harvesting) than does optimized isobaric actuation.

Figure S3 shows the air temperature in close proximity to an actuating, fully-heated coiled SZ fiber and the resulting rotation of a magnetic rotor as a function of time following the delivery of a pulse of hot air. Note the time lag between measured air temperature and the peak in rotation angle, which is near zero for an air temperature change of 25.1°C and 45.5°C and about 20 ms for $\Delta T = 63.2^\circ\text{C}$ and 71.2°C .

The cycle life evaluation shown in Fig. 3c was obtained by mechanizing the periodic delivery of hot air pulses to the muscle fiber. For this purpose, a quadrant of a circular insulating board was cut away, thereby providing a fan shape board that was rotated by a stepper motor. The board was between a heat gun and the muscle, with the cut-out segment aligned with the heat gun and muscle, thereby enabling periodic exposure of the muscle to hot air. The cycle rate of the stepper motor was 3 Hz and the heating time (exposure time)

was 0.083 seconds, while the cooling time (blocked time) was 0.25 seconds during each cycle. With this system, it is difficult to match the heating/cooling period with the untwisting/retwisting period of the torsional muscle. Hence, the data in the Fig. 3 inset was obtained by shaking the heat gun by hand until the resonance frequency was manually obtained.

Figure S4(b), which is again for a coiled 27- μm -diameter fiber and the magnetic rotor of this section, shows the dependence of percent tensile actuation and torsional rotation angle on time for different applied tensile loads during isobaric actuation of a coiled half-heated ZZ fiber. For reference, the time dependence of air temperature at the muscle is also provided. For low applied loads, tensile actuation is near zero, since coils are either contacting at ambient temperature (which is the case for 26 MPa load) or nearly contacting (for 36 MPa load), which interferes with thermal contraction. Nevertheless, although this contact reduces torsional rotation to near zero for 26 MPa load (which was the load applied during muscle fabrication), there is sufficiently low inter-coil friction for large torsional rotation to result for 36 MPa load and for 53 MPa and 70 MPa loads, where in the latter cases tensile contraction is essentially unimpeded by inter-coil contact. Figure S4(c) shows the dependence of peak gravimetric rotor kinetic energy and tensile work capacity during contraction on ΔT for a tensile load of 53 MPa. The length of the coiled ZZ fiber (after loading with 53 MPa stress) was 95 mm.

3.2 Electricity generation using torsional muscle

The generator of Fig. S5 uses a fully-heated, coiled SZ fiber (made by inserting twist in a 27- μm -diameter nylon 6,6 precursor fiber to provide a 95 mm-long coiled polymer muscle that weighed 0.25 mg) to rotate a magnetic rotor (NdFeB-N50, with a moment of inertia of $8.97 \times 10^{-13} \text{ kg}\cdot\text{m}^2$) that induces current in two nearby metal wire coils. These wire induction coils were from the watch mentioned in Section 2. The two metal wire coils were connected in series for increasing the generated voltage two-fold, electrical power and electrical energy. The generated voltage on the metal wire coil was measured by an oscilloscope using a 10 megaohm impedance probe. Following application of a warm air pulse that increased temperature 65°C , the output electrical voltage and electrical power generated across a load resistor R_L (see Fig. S5c inset circuit) was measured. The peak electrical power output (0.144 mW, corresponding to 0.576 W/g of muscle) was obtained when the external load resistance was 6.4 k Ω . This generated voltage can be also rectified using the electrical circuit (Fig. S5a circuit diagram) and the rectified voltage can deposit electrical energy into a 330 μF -10V capacitor using a sequence of hot air pulses (providing a temperature peak of 90°C) that were provided every 0.2 seconds. The voltage on the capacitor reached 1.15 V after 35 seconds. Based on the 330 μF capacitance of the capacitor, the maximum capacitor voltage attained, the charging time, and the 0.25 mg muscle weight, the average electrical power delivered by the generator and associated circuit of Fig. S5 was 24.9 W/kg. The lower average power delivered to the capacitor, compared with the 38.1 W/kg average power delivered to external resistors, is likely a result of energy losses in the Fig. S5 (a) circuit used for capacitor charging and imperfect impedance matching to this circuit.

Figure S6 provides the time dependence (from top to bottom) of air temperature, open-circuit voltage, closed-circuit voltage, electrical power and harvested electrical energy when using a single hot-air pulse providing a temperature change of 65°C . The results are for the load resistance that maximizes output power (both instantaneous and average). The Fig. S6a results are for the experiment of Fig. 4 on a fully-heated, isometrically actuated, coiled SZ fiber made from a 102- μm -diameter nylon 6,6 precursor fiber (where the electrical output of only one of the three wire coils is shown). Figure S6b shows results for the experiment of

Fig. S5a-c on a fully-heated, coiled SZ, 27- μm -diameter fiber that was isometrically actuated, where the voltage is that provided by two wire coils connected in series to harvest energy from the torsional rotation of the magnetic rotor. The moment of inertia of the magnetic rotor was reduced by a factor of 3190 (corresponding to a moment of inertia decrease from $2.86 \times 10^{-9} \text{ kg}\cdot\text{m}^2$ to $8.97 \times 10^{-13} \text{ kg}\cdot\text{m}^2$) as the diameter of the precursor fiber was reduced from 102 μm diameter to 27 μm diameter.

Figure S7 shows that greatly increased electrical power generation can be obtained by providing hot air pulses at the resonance-frequency of the torsional energy harvester. Using the setup of Figure S5a (for a 95-mm-long coiled fiber weighing 0.25 mg, made from a 27- μm -diameter precursor fiber, and a load resistance of 6.4 k Ω), a ΔT fluctuation of 19.6 $^\circ\text{C}$ (from 67.6 $^\circ\text{C}$ to 87.2 $^\circ\text{C}$) at 4.8 Hz provided 6.48 $\mu\text{J}/\text{cycle}$ at this frequency, which corresponds to 25.9 J/kg of muscle weight. The average power output per muscle weight was 124 W/kg for the used air temperature fluctuation of 19.6 $^\circ\text{C}$, which produced a 70,000 rpm peak rotor speed.

Figure S8 shows resonant energy harvesting at closer to room temperature for a fluctuation of air temperature of 8.2 $^\circ\text{C}$ (from 32.5 $^\circ\text{C}$ to 40.7 $^\circ\text{C}$ at ~ 5 Hz) using the setup of Figure S5a and the above coiled muscle fiber and load resistance. For one cycle (lasting ~ 0.2 second), the muscle generated 1.34 $\mu\text{J}/\text{cycle}$, which corresponds to 5.35 J/kg of muscle weight. The muscle provided a peak torsional speed of 33,000 rpm, a peak output voltage of 0.46 V, a peak output power per muscle weight of 132 W/kg, and average power per muscle weight of 26.8 W/kg for this 8.2 $^\circ\text{C}$ fluctuation in air temperature. Note that an approximately quadratic dependence of output electrical energy per cycle on ΔT is supported by comparison of Fig. S7 and Fig. S8 results, since the ratio of output energy/cycle for a ΔT of 19.6 $^\circ\text{C}$ to that for a ΔT of 8.2 $^\circ\text{C}$ (4.83) approximately equals the ratio of the squares of the corresponding ΔT values (5.7). Furthermore, note that that ratio of average electrical output power for these different values of ΔT gives about the same ratio (4.6).

Figure S9 describes the electrical circuit that was used for powering the light emitting diodes shown in Figure 4d.

Figure S10 shows the use of artificial muscle torsional actuation to switch on-and-off the delivery of hot air, so that this same muscle can be used to rotate a magnetic rotor that is used for harvesting electrical energy. A baffle was attached near the bottom of a coiled fully-end-tethered SZ fiber, which had a NdFeB-N50 magnet (moment of inertia of $8.97 \times 10^{-13} \text{ kg}\cdot\text{m}^2$) attached at fiber midpoint. The rotating half-moon baffle alternatively deflected and transmitted the flow of hot air through the half-moon orifice from the underlying continuously-operated heat gun. The baffle interrupted air flow every 5 turns of the magnetic rotor, providing a hot air pulse frequency of 6 Hz. The coiled SZ fiber was 95-mm-long and made by twisting a 27- μm -diameter precursor nylon 6,6 fiber.

By using a fan without a heater, we evaluated the effect of room temperature air current on paddle rotation and resulting generation of electrical energy. Independent of the direction from which we delivered the air flow or whether or not the air flow was pulsed, there was no noticeable resulting rotation of the magnetic rotor and little movement of this rotor. This result is not surprising considering the high mass of the rotor compared to the cross-sectional area that would result in interaction with air flow. Consequently, no significant voltage (less than 1 mV) was produced by exposure of the magnetic rotor to room temperature air current. In contrast, the experiment using periodically interrupted hot air flow (Fig. S10) resulted in a quite large maximum torsional rotation speed (about 10,000 rpm), as well as a peak voltage of 40 mV.

4. Efficiencies of mechanical to electrical energy conversion

Even if we ignore energy exchange between tensile and torsional energies, calculation of energy conversion efficiency is complicated due to the changing temperature and contributions of both increasing and decreasing energy to the kinetic energy of the magnetic rotor. A lower limit on the efficiency of conversion of torsional kinetic energy into electrical energy was calculated from equation (1):

$$\text{Efficiency } (\eta) > \frac{3 \int_{t_1}^{t_2} V^2 / R \, dt}{\sum_1^n \frac{1}{2} I \cdot \omega_n^2}, \quad (1)$$

where V is the generated voltage, I is the rotor's moment of inertia, t_1 and t_2 are the start and finish times of total voltage output, and ω_n is the n -th peak of torsional angular velocity when the generator is operated open circuit. For calculation of the upper limit estimate of energy conversion efficiency, the denominator in equation (1) is replaced by $\frac{1}{2} I (\omega_{\max})^2$, where ω_{\max} is the maximum torsional angular velocity. The thereby calculated efficiency for mechanical-to-electrical energy conversion is $43.6 < \eta < 97.2\%$ for the three coil generator of Fig. 3 and Fig. S6a and $15.8\% < \eta < 43.7\%$ for the two coil generator of Fig. S6b.

As shown in Fig. 5b for the tensile harvester, the energy conversion coefficient (the ratio of output electrical energy to the mechanical work done by lifting the weight in the harvester) increased monotonically with decreasing load, reaching 35% for 18 MPa load. This energy conversion coefficient for the tensile muscles underestimates the true obtained efficiency for converting thermally harvested mechanical energy to electrical energy, since the mechanical work done to lift a weight during muscle contraction overestimates the work that can be done during a complete work cycle.

5. Theoretical Calculations

5.1 Scalability of tensile and torsional actuation

Our previous experimental results¹ showed that the tensile stroke per muscle length and the specific work capacity during contraction for coiled nylon 6 muscles did not significantly change as the diameter of the precursor fibers varied between 150 μm and 2.45 mm, as long as the applied stress during twist insertion and the applied stress during actuation were both kept constant (when normalized with respect to the cross-sectional area of the precursor fiber). The near-invariance of these actuator properties indicated that the precursor fibers had nearly the same structure and relevant thermal, mechanical, and thermo-mechanical properties and that the severe deformations during twist insertion maintained the equivalence of structure and resulting properties over this 267-fold range in cross-sectional area. This scalability of structure automatically occurs during twist insertion, so that the fiber bias angle at just below the point of coiling and the product of the number of coils per precursor fiber length and the precursor fiber diameter are scale invariant. Also, the observed product τD (where τ is the turns/meter of inserted twist and D is the precursor fiber diameter) is independent of scale for both the fiber just before the point of coiling and after the point of complete coiling.

Since calculation of fiber torsional actuation by such methods as finite element analysis involves unknown quantities (the dependence of the elasticity tensor for each finite element on temperature and local polymer bias angle, and the dependence of anisotropic thermal expansion on these quantities), we cannot presently predict the temperature dependence of steady-state torsional or tensile stroke or the specific work capacity of these

actuation processes. Nevertheless, unless the precursor fiber diameter is on the nanoscale, the above scalability of structure implies that finite element calculations would predict the scalability of tensile and torsional actuation for both twisted and coiled polymer muscles. The point here is that finite elements that are identical in properties (but scaled in size according to the precursor fiber diameter) can be chosen independent of the magnitude of this diameter. Hence, the finite element calculations should predict scalability of both torsional and tensile actuation. This means that the equilibrium specific work capacity during tensile or torsional actuation should be scale invariant. The observed independence of specific tensile work on muscle diameter for coiled muscles¹ supports these arguments. Also, theory and observation show that the percent tensile stroke of the coiled muscle is proportional to the product of torsional stroke per length of the twisted muscle and the number of coils per muscle length, which indicates that the product of the precursor fiber diameter and the torsional stroke of the twisted fiber per fiber length is scale invariant.

5.2 The dependence of peak rotor kinetic energy on the moment of inertia of the rotor

The experimental results of Fig. 2 b, c show that the peak rotor kinetic energy is independent of the moment of inertia of the rotor. In order to theoretically verify this dependence, the dynamics of the rotor assembly is described by

$$I\ddot{\theta} + 2I\xi\omega_0\dot{\theta} + k_\theta\theta = Q,$$

where Q is the thermally generated torque, I is the rotational moment of inertia of the rotor, θ is the torsional angle of the rotor, ξ is the damping ratio (representing mechanical energy dissipation by conversion to heat and/or electrical energy), $\omega_0=(k_\theta/I)^{1/2}$ is the natural torsional oscillation frequency, and k_θ is the torsional spring constant of the system.

At $t=0$, the system is perfectly balanced, with an initial torsional angle and torsional velocity of 0. Assuming that the thermally-generated torque is $Q=T_0\sin(\omega t)$, the steady-state solutions for the torsional angle and speed are²:

$$\begin{aligned}\theta &= T_0 \sin(\omega t - \phi) / (k_\theta H(\Omega)) \quad \text{and} \\ \dot{\theta} &= T_0 \omega \cos(\omega t - \phi) / (k_\theta H(\Omega)),\end{aligned}$$

where $\phi = \tan^{-1}(2\xi\Omega/(1-\Omega^2))$, $H(\Omega) = ((1-\Omega^2)^2 + (2\xi\Omega)^2)^{1/2}$ and $\Omega = \omega/\omega_0$. The peak rotor kinetic energy corresponds to the peak angular velocity, which can be obtained from the above by applying $\omega \rightarrow \omega_0$ and letting $\cos(\omega t - \phi) = 1$. Hence, the rotor speed that provides the maximum rotor kinetic energy is

$$\dot{\theta}_{\max} = T_0 \omega_0 / (2\xi k_\theta)$$

This equation shows that $\dot{\theta}_{\max}$ is proportional to ω_0 . Since $\omega_0 = (k_\theta/I)^{1/2}$, we obtain $\dot{\theta}_{\max} \sim I^{-1/2}$. Hence, since the peak kinetic energy is $I\dot{\theta}_{\max}^2/2$, this peak torsional energy is independent of the moment of inertia of the rotor.

5.3 Further analysis of the scaling of torsional actuation

Scaling effects on torsional actuation can be estimated by combining the above relations for peak kinetic energy (W_{\max}) as:

$$W_{\max} = \frac{2T_0^2}{k_\theta}$$

since $W_{\max} = \frac{1}{2} (\theta_{\max})^2 I$ and $\theta_{\max} = \frac{2T_o}{k_{\theta}^{1/2} I^{1/2}}$ when the damping ratio $\xi = 1$. The torsional spring constant of the fiber of circular cross-section and diameter D and length L is:

$$k_{\theta} = \frac{\pi D^4 G}{32L},$$

where G is the shear modulus of the fiber material. Since the maximum rotation is $\theta_{\max} = T_o/k_{\theta}$, the maximum work output will be:

$$W_{\max} = 2\theta_{\max}^2 k_{\theta} = \frac{\pi D^4 G}{16L} \theta_{\max}^2$$

and normalised to fiber volume (V):

$$\frac{W_{\max}}{V} = \frac{D^2 G}{4L^2} \theta_{\max}^2$$

Experimentally it has been found that the maximum fiber rotation decreases with fiber diameter for twisted nylon 6 fibers prepared with the same outer bias angle ($\alpha=30^\circ$) and heated over the same temperature range (Fig. S11a). The maximum rotation angles scales with the inverse of fiber diameter (Fig. S11b), which can be understood if maximum rotation depends on the amount of twist inserted (τ , turns per fiber length) and fiber length: $\theta_{\max}=KL\tau$ (where K is a constant). The bias angle is related to the inserted twist and fiber diameter as $\tan\alpha = \pi\tau D$, so that:

$$\theta_{\max} = \frac{KL \tan \alpha}{\pi D}$$

Combined with the above expression gives:

$$\frac{W_{\max}}{V} = \frac{K^2 G \tan^2 \alpha}{4\pi^2}$$

From which it can be seen that volumetric work capacity is scale-independent for fibers twisted to a constant bias angle.

References

1. Haines, C. S. *et al.* Artificial muscles from fishing line and sewing thread. *Science* **343**, 868-872 (2014).
2. Rao, S.S. Mechanical vibrations. Vol. 4. New York: Addison-Wesley, 1995.

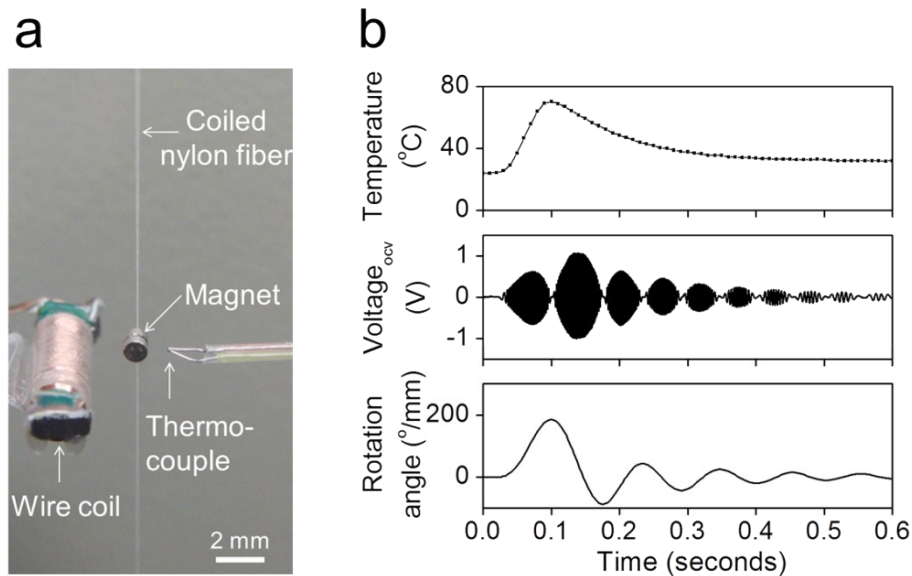


Figure S1. Apparatus for the electromagnetic measurement of thermally driven torsional rotation of a muscle fiber. **a**, Photograph showing the positioning of a torsional muscle fiber (whose midpoint supports a magnetic rotor), a thermocouple, and a wristwatch coil used for sensing. Temperature change induced by a warm air pulse causes muscle driven torsional rotation of the magnet, which generates voltages in the wire coil that are recorded on an oscilloscope. The rotation angle and torsional speed of fiber are calculated from the observed voltage signal. **b**, Typical time profiles of temperature, generated voltage, and derived rotation angle for a fully two-end-tethered coiled SZ fiber that has been driven by one pulse of warm air. The magnet has a moment of inertia of $8.97 \times 10^{-13} \text{ kg} \cdot \text{m}^2$ and the coiled muscle fiber (made from a $27\text{-}\mu\text{m}$ -diameter precursor nylon 6,6 polymer fiber) was 75 mm long.

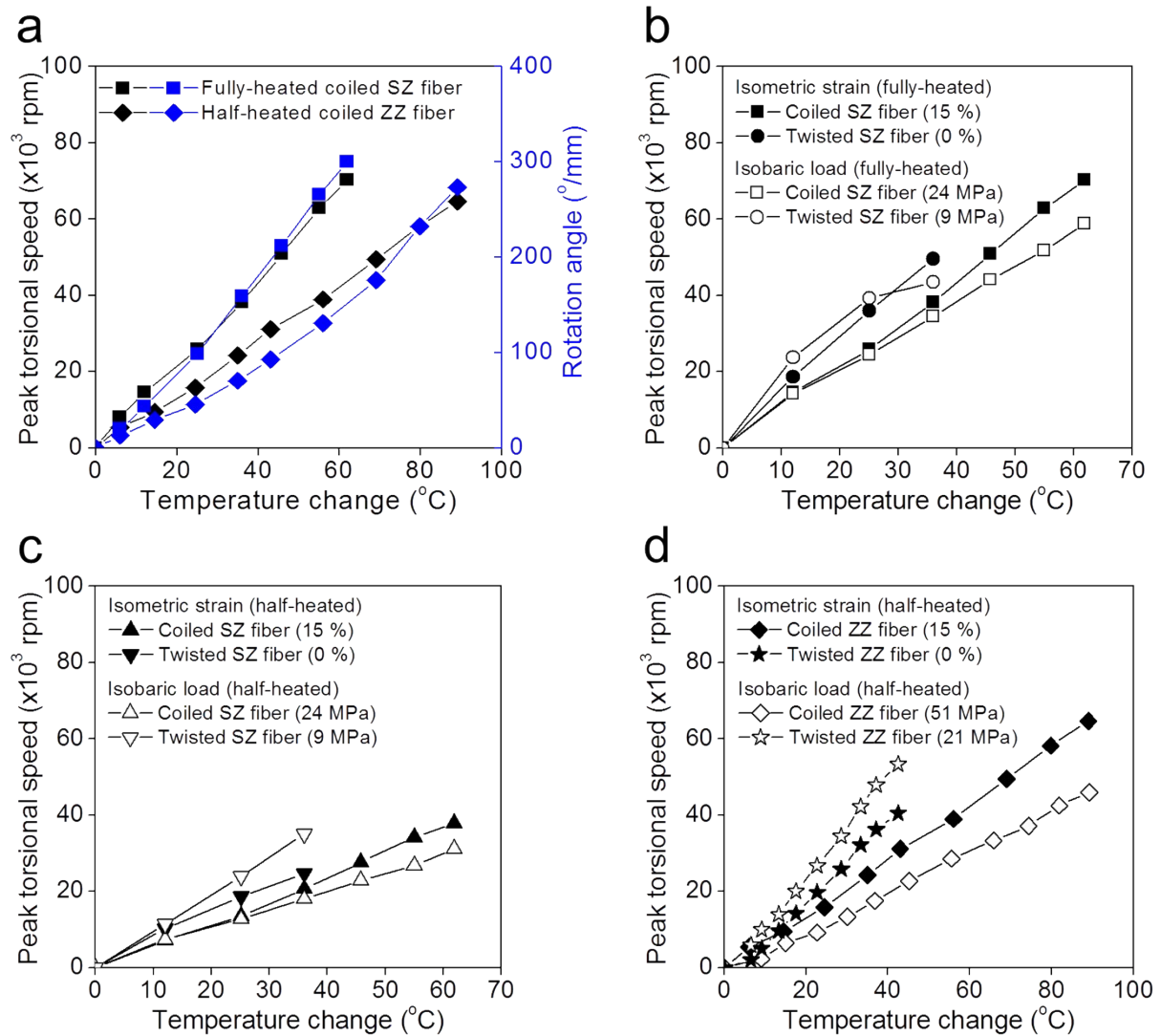


Figure S2. Peak rotor torsional speed and maximum rotation angle as a function of air temperature change (ΔT) produced by a hot-air pulse for optimized isometric (closed symbols) and isobaric (open symbols) actuation. a, Dependence of peak rotor speed (black symbols) and maximum rotation angle (blue symbols) on ΔT for fully-heated coiled SZ fiber (squares) and one-half-heated coiled ZZ fiber (diamonds) that are isometrically stretched by 15%. **b,** Dependence of peak rotor speed on ΔT for coiled SZ fiber (squares) and twisted SZ fiber (circles) that are fully heated. **c,** Dependence of peak rotor speed on ΔT for a coiled SZ fiber (triangle) and a twisted SZ fiber (inverted triangle) that are one-half heated. **d,** Dependence of peak rotor speed on ΔT for a coiled ZZ fiber (diamonds) and a twisted ZZ fiber (stars) that are one-half heated.

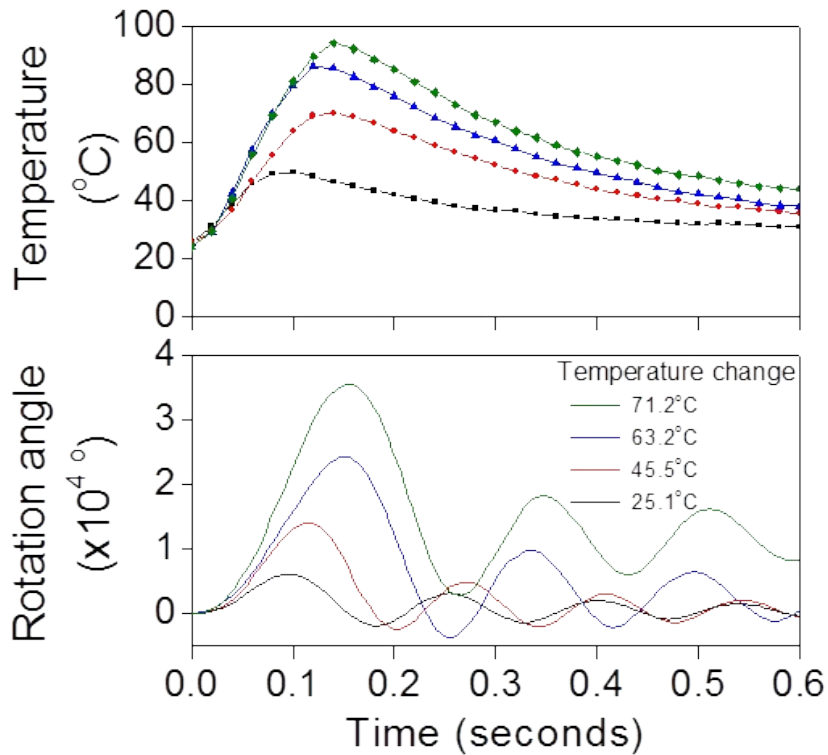


Figure S3. Time dependence of rotation angle and temperature for a coiled SZ fiber during heating with a pulse of hot air. Temperature changes of 25.1°C (black), 45.5°C (red), 63.2°C (blue), and 71.2 °C (green) were used for the fully-heated, coiled SZ fiber. The magnetic NdFeB-N50 rotor, which was attached at fiber centre, had a moment of inertial of $8.97 \times 10^{-13} \text{ kg} \cdot \text{m}^2$. The diameter of the precursor fiber was 27 μm , the length of the coiled fiber after stretching was 75 mm, and this coiled fiber was stretched 15% before isometric actuation measurements.

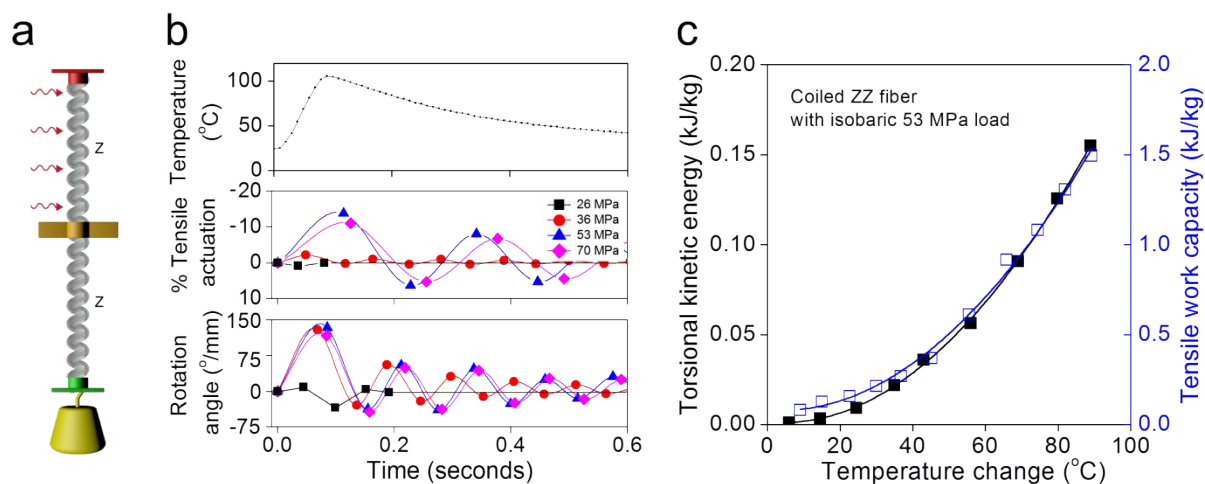


Figure S4. Characterization of the tensile and torsional dynamics and energetics of a half-heated coiled ZZ fiber during isobaric actuation produced by a pulse of warm air. **a**, The configuration used for measuring actuation, where extreme fiber ends are torsionally tethered and only the top ZZ yarn segment is heated. **b**, The time dependence of tensile actuation and torsional actuation for the ZZ fiber for different applied stresses (indicated in the inset, where stresses were normalized to the area of the precursor nylon 6,6 fiber). The initial positive rotation direction corresponds to fiber untwist for all loads, while tensile actuation shows a very small expansion for 26 MPa load and larger contractions for 36, 53, and 70 MPa loads. This anomalous expansion for 26 MPa load results since coil insertion occurred at 26 MPa load and such load resulted in contacting coils that prohibit yarn contraction. **c**, The dependence of maximum torsional kinetic energy density (derived from the maximum rotation speed) and the tensile work capacity during contraction on pulsed temperature change when the isobaric load was 53 MPa. The initial diameter of the nylon fiber before processing was 27 μm and the length of the coiled ZZ fiber (after loading with a weight) was 95 mm. The magnetic NdFeB-N50 rotor used, which was attached at fiber centre, had a moment of inertia of $8.97 \times 10^{-13} \text{ kg} \cdot \text{m}^2$.

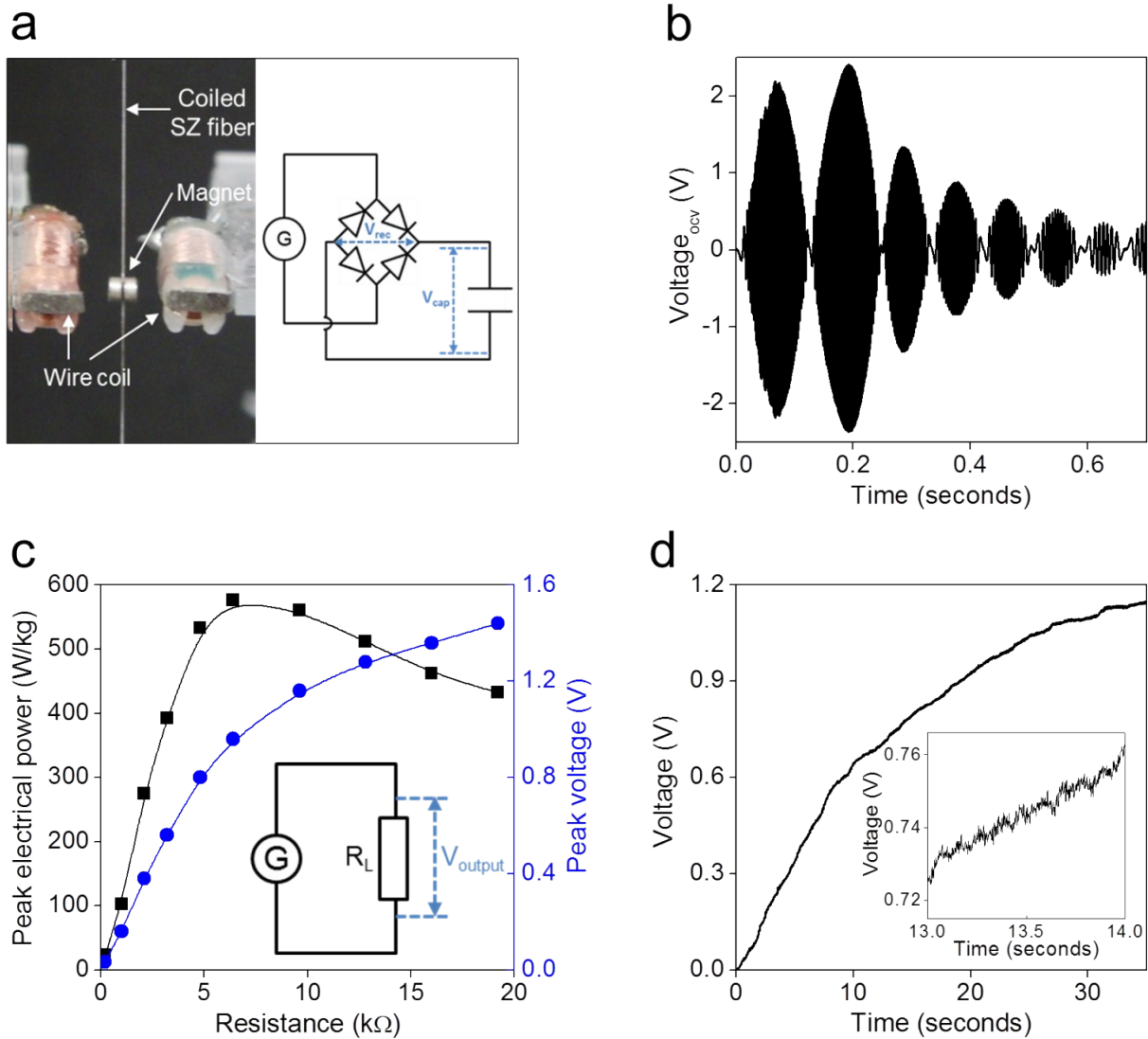


Figure S5. Electricity generation using torsional muscle actuation driven by fluctuations in air temperature for a fully-heated, coiled SZ, 27- μm -diameter fiber. **a**, The photograph (left) shows one of the configurations used for harvesting electrical energy from torsional actuation generated by fluctuations in air temperature. The diagram on the right shows the rectifying diode circuit used for storing harvested electrical energy in a capacitor. **b**, The time dependence of the open circuit voltage on the wire coil, as measured by an oscilloscope, following application of a pulse of warm air that produced a 65°C temperature increase above ambient temperature. **c**, The peak output electrical power (black squares) and peak voltage (blue circles) as a function of the load resistance R_L applied to the series-connected coils (see inset circuit) following application of a warm air pulse that increased temperature 65°C . The peak electrical power output (0.144 mW , corresponding to 0.576 W/g of muscle) was obtained when the external load resistance was $6.4\text{ k}\Omega$. **d**, The time dependence of capacitor voltage when charging a $330\text{ }\mu\text{F}$ - 10V capacitor (see the circuit diagram in the inset of **a**) using warm air pulses (providing a temperature peak of 90°C) that were provided every 0.2 seconds during 35 seconds.

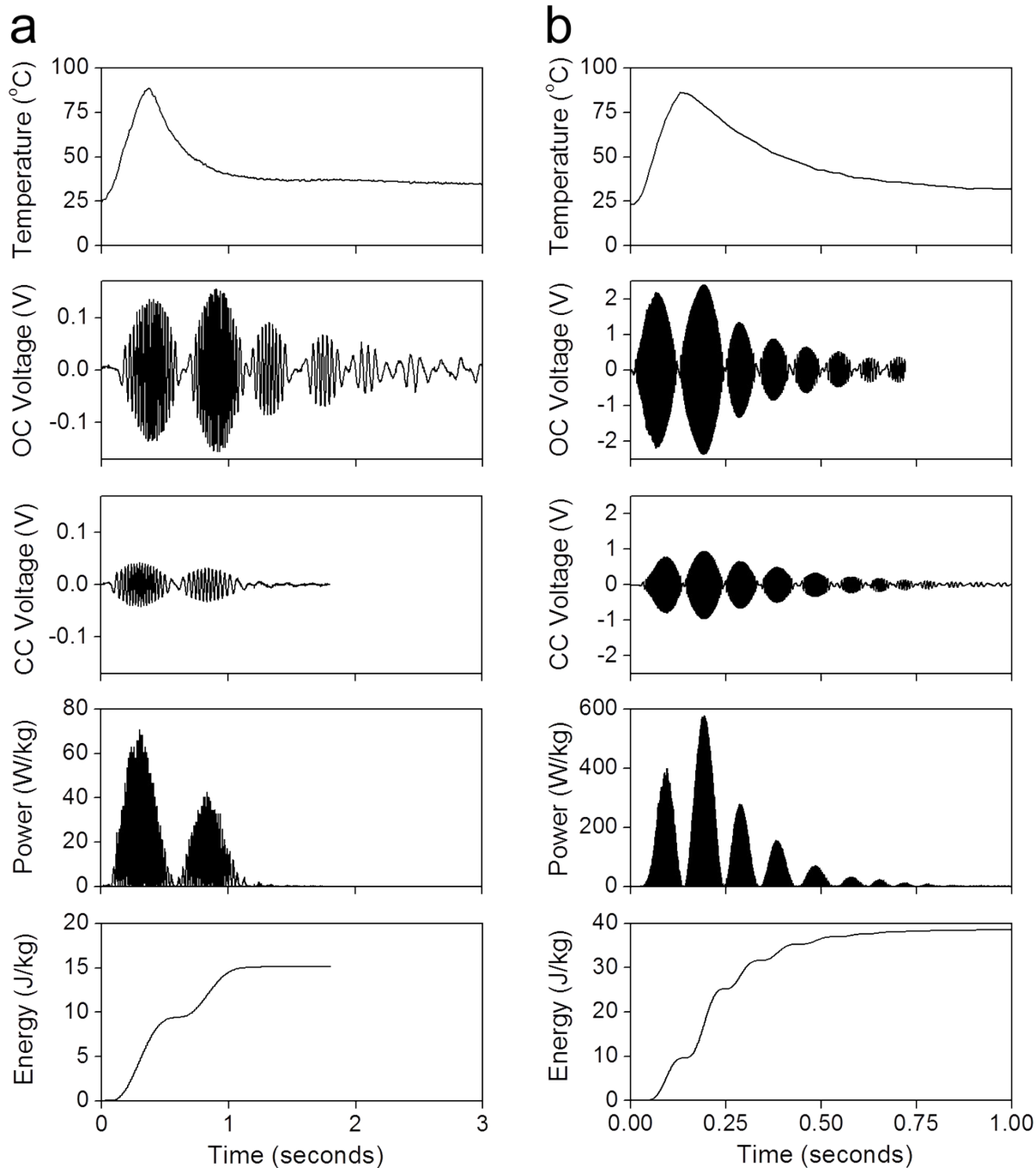


Figure S6. The time dependence (from top to bottom) of air temperature, open circuit (OC) voltage, closed circuit (CC) voltage, output electrical power, and harvested electrical energy when using a single hot-air pulse providing a temperature change of 65°C. **a**, The experiment of Fig. 4 on a fully-heated, isometrically-actuated, coiled SZ fiber from a 102- μm -diameter nylon 6,6 precursor fiber (where the voltage, power, and energy plots are for one of the three identical wire coils that harvest energy) and **b**, Results for a fully-heated, coiled SZ, 27- μm -diameter fiber that was isometrically actuated, where the voltage is that of two series-connected wire coils.

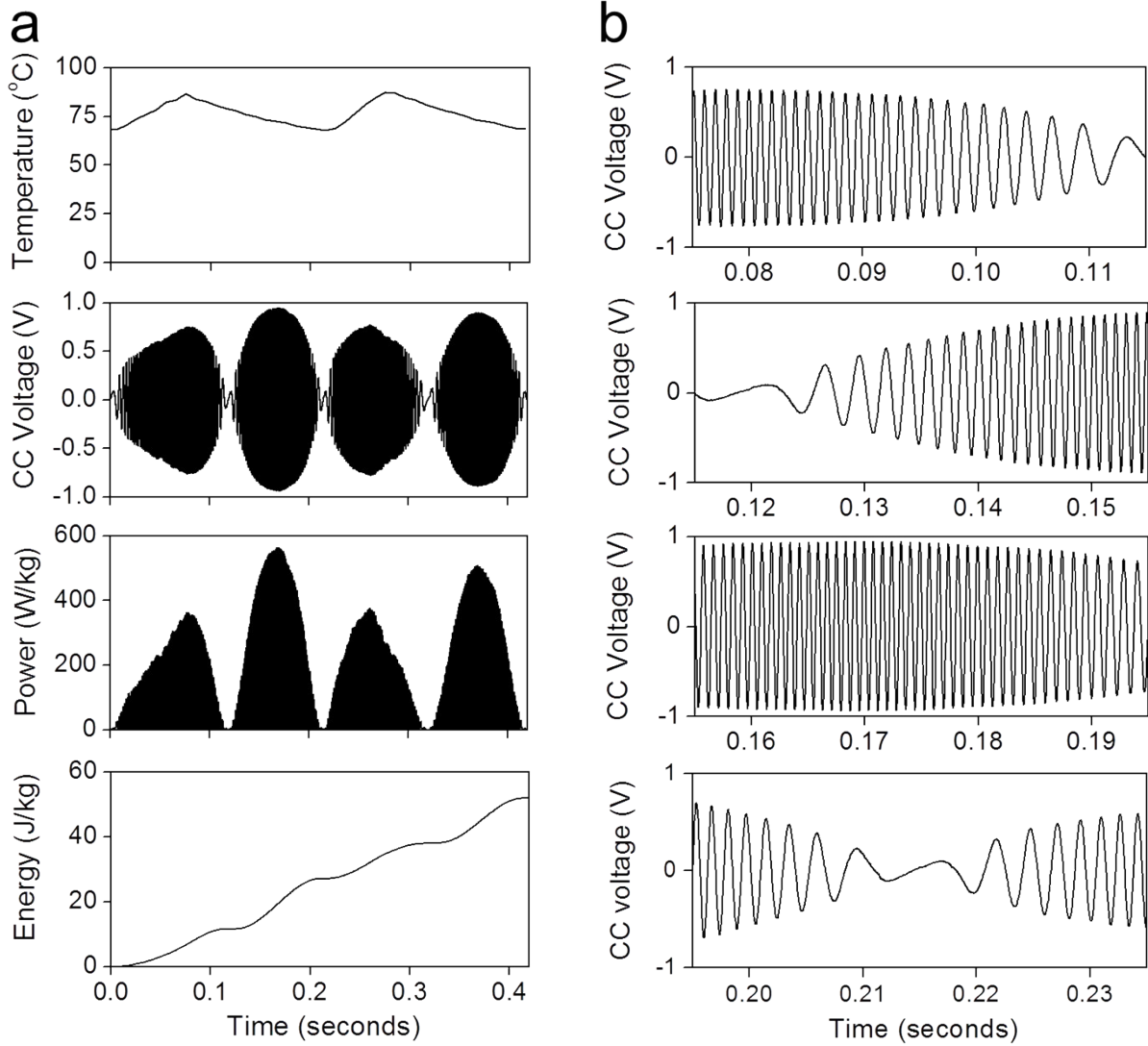


Figure S7. Electrical voltage and power generated by matching the frequency of the thermal cycle to the mechanical resonance frequency, using the setup of Figure S5a. a. Results for a fully-heated, coiled SZ, 27- μ m-diameter fiber that was isometrically actuated, where the voltage is that of two series-connected wire coils. **b.** An expanded view for the pulses during cooling.

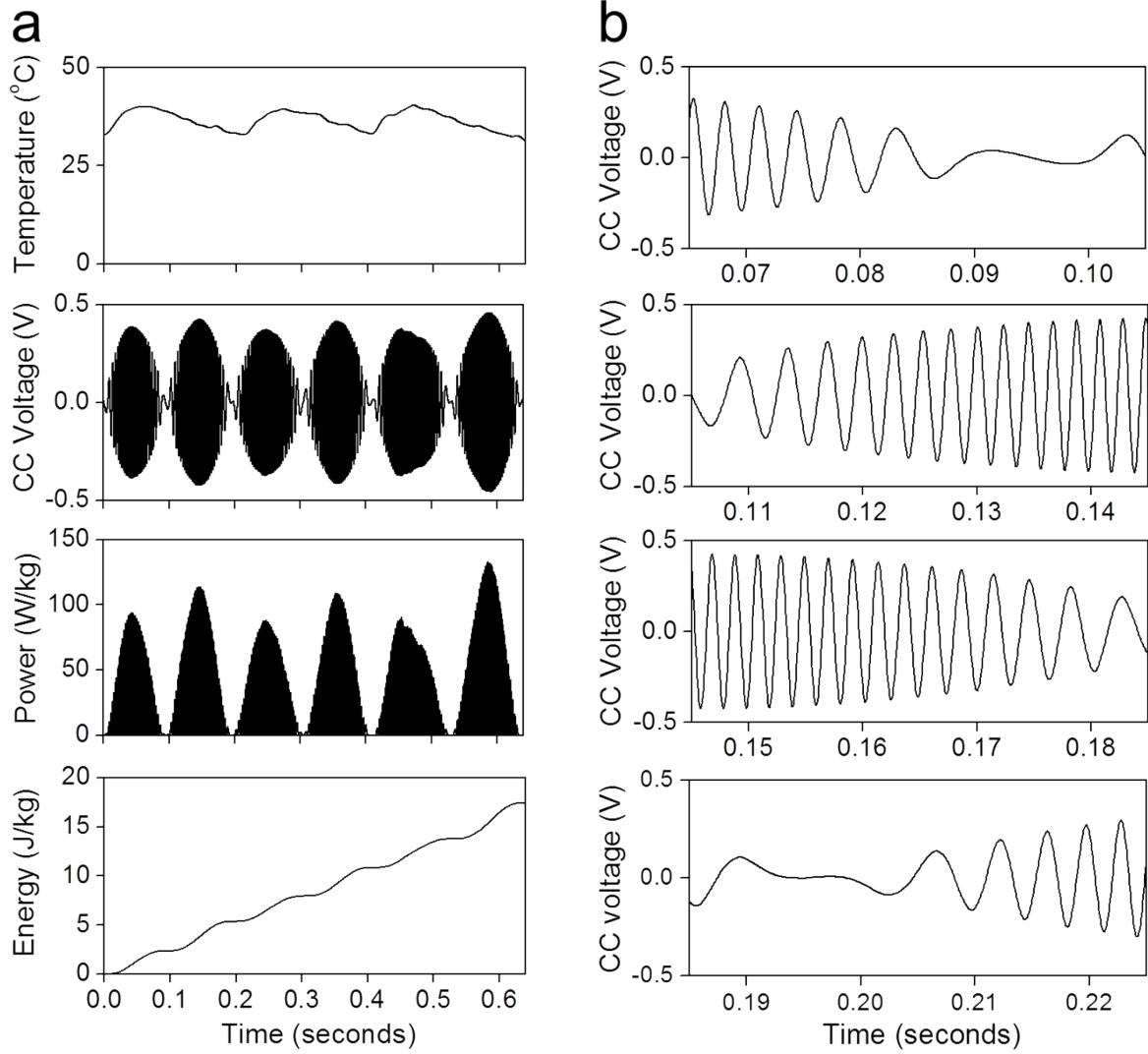


Figure S8. Resonant energy harvesting at near room temperature for a ΔT of ~ 8.2 °C. a. Results for a fully-heated, coiled SZ, 27- μm -diameter fiber that was isometrically actuated, where the voltage is that of two series-connected wire coils using the setup of Figure S5a. **b.** An expanded view for the pulses during cooling.

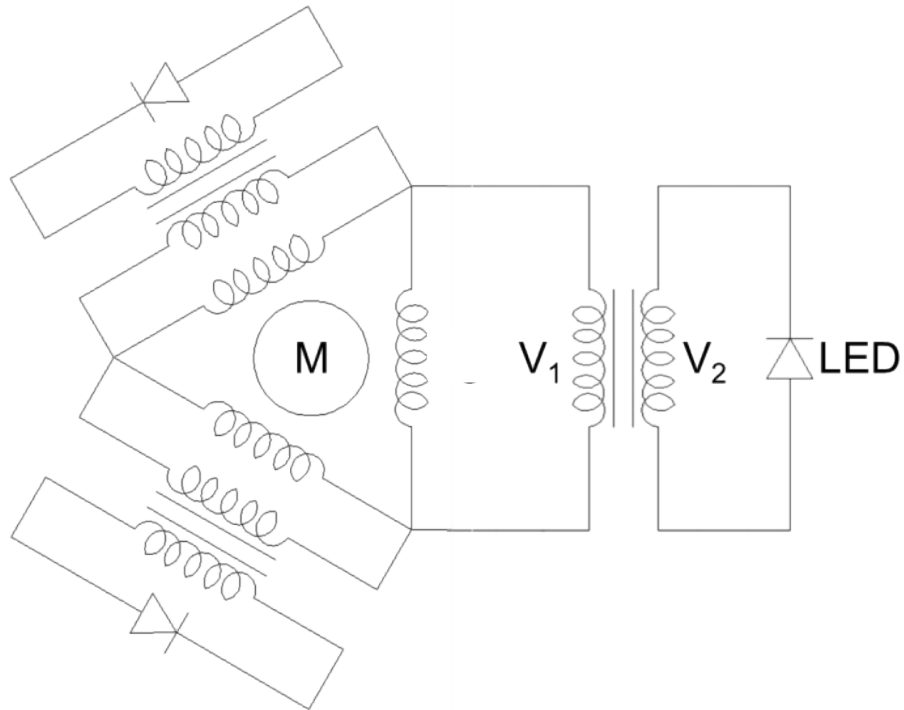


Figure S9. The circuits used for harvesting the electricity produced by each phase of the magnetic generator and amplifying it for lighting the three LEDs. The generator shown in Fig. 4a produced the three-phase alternating current oscillating output voltages (Fig. 4b) with a maximum open-circuit (single-phase voltage) of 0.16 V (V_1). This output from each of the three phases is smaller than the forward voltage needed for operating each of the LEDs, so three step-up transformers were used to amplify the output voltage from each phase output (V_1) 18 times to 2.8 V (V_2). (M: magnetic rotor, V_1 : output voltage from each phase of the generator, V_2 : amplified voltage from transformer).

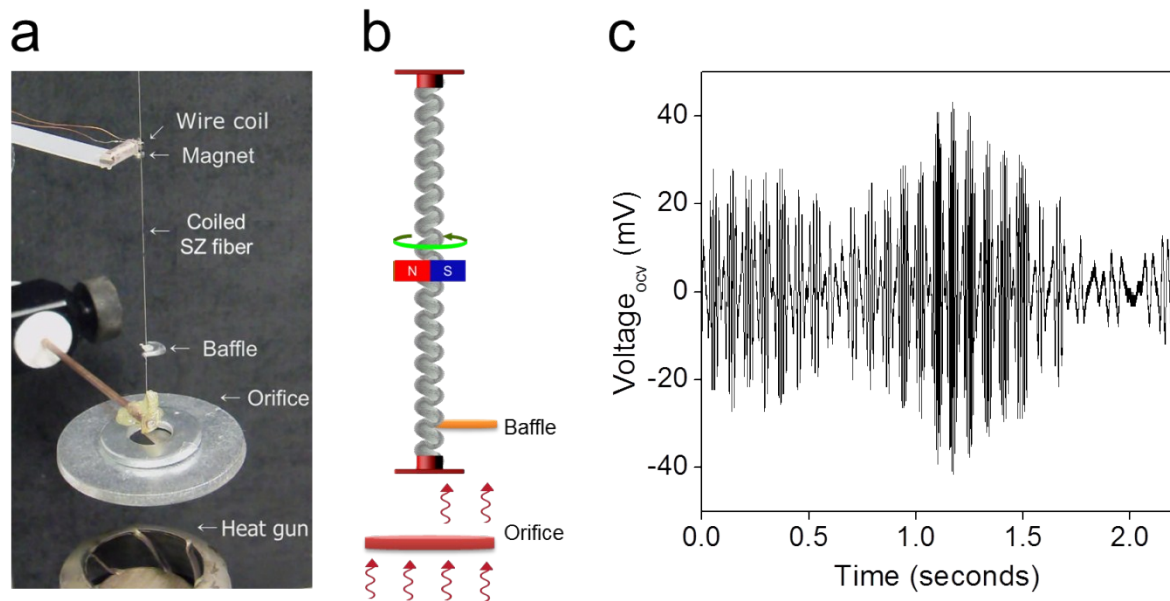


Figure S10. Use of a muscle-powered rotating baffle for converting a continuous stream of warm air to the oscillating warm air pulses needed for continuous electrical energy harvesting. **a**, Photograph and associated component labels showing the setup used for exploiting torsional actuation for pulsing a continuous flow of warm air, and using the thermal pulses for electromagnetically harvesting thermal energy. A baffle was attached near the bottom of a coiled fully-end-tethered SZ fiber, which had a magnetic NdFeB-N50 rotor (having a moment of inertia of $8.97 \times 10^{-13} \text{ kg}\cdot\text{m}^2$) attached at fiber midpoint. The rotating half-moon baffle alternatively deflected and transmitted the flow of hot air through the half-moon orifice from the underlying continuously-operated heat gun. **b**, Schematic illustration showing the torsionally actuating components of the system pictured in **a**. **c**, The time dependence of open circuit voltage from the generator shown in **a**. The baffle interrupted air flow every 5 turns of the magnetic rotor, providing a warm air pulse frequency of 6 Hz. The coiled SZ fiber used was 95-mm-long and made by twisting a 27- μm -diameter precursor nylon 6,6 fiber.

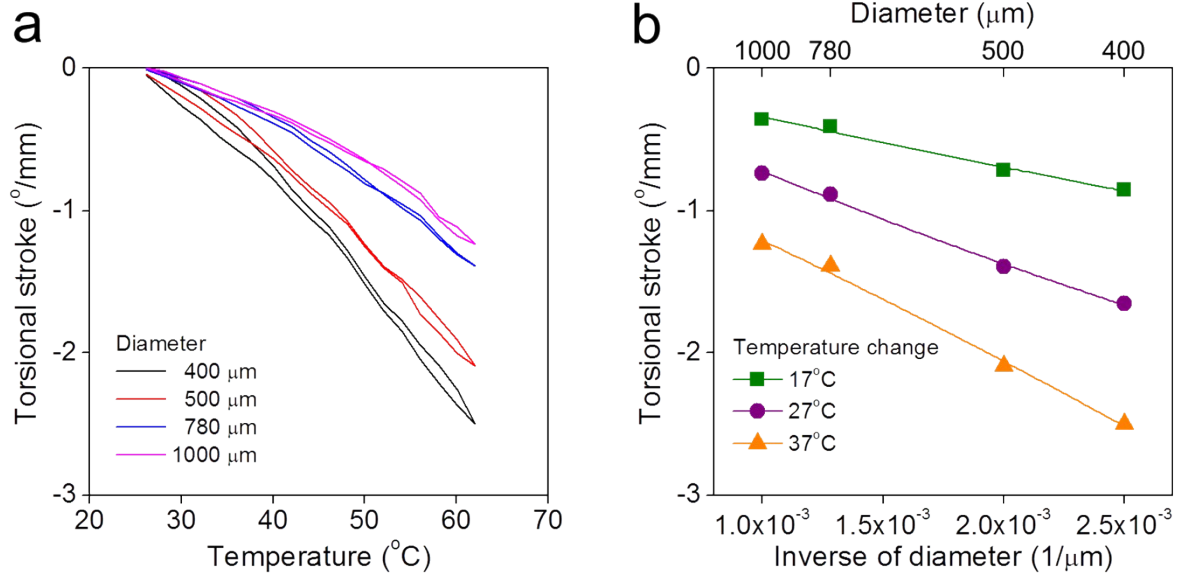


Figure S11. Steady-state torsional actuation for a one-end-tethered, twisted nylon 6 monofilament fishing line heated at 3.6 $^{\circ}$ C/min and cooled at 1.8 $^{\circ}$ C/min over a temperature range of 26-62 $^{\circ}$ C. Four different diameter fibers were used, which were all twisted to a bias angle of 30 $^{\circ}$. a, Torsional stroke per muscle length as a function of fiber temperature. b, Torsional stroke as a function of fiber diameter and inverse diameter for 3 different temperature ranges of 17 $^{\circ}$ C (green), 27 $^{\circ}$ C (purple), and 37 $^{\circ}$ C (orange).

Supplementary Video (S1-S4) Captions

Video S1. Powering light-emitting diodes using a torsional energy harvester

A pulse of hot air delivered to a heterochiral, coiled nylon 6,6 muscle generates a 65°C temperature change, which sequentially rotates a magnetic rotor in fiber untwist and retwist directions. A miniature 3-phase generator harvests the resulting torsional energy of the magnetic rotor as electrical energy, which lights the three diodes (first during fiber untwist and then during fiber retwist). This process is then repeated for the used, 95-mm-long, coiled 106- μm -diameter, nylon torsional muscle.

Video S2. Self-regulated torsional actuation in a draft of warm air

A draft of 60°C hot air, automatically turned on and off by an rotating pin, drives the continuously repeated untwist and twist of a coiled heterochiral nylon muscle that torsionally rotates a magnetic rotor. The 23- μm -diameter, 95-mm-long nylon 6,6 muscle torsionally rotates the pin over a much smaller rotation angle and at a much lower frequency than the magnetic rotor, so that sections of the torsional muscles are alternately heated and cooled. A voltage induced in a wire coil is used to measure magnet rotation.

Video S3. Light-emitting diodes powered by electricity generated by rotation of motor using the thermally generated tensile actuation of four parallel, coiled, 1-mm-diameter polyethylene fibers

Video S4. Characterization of torsional actuation produced by temperature fluctuations

Characterization of thermally powered torsional actuation produced by three pulses of hot air, which were periodically delivered from the right by a hot air gun (after rotation stopped). The wire coil (on the left of the magnetic rotor) sensed rotation speed, thereby providing the displayed signal. The used 75-mm-long coiled heterochiral nylon muscle (made from 23- μm -diameter precursor fiber) twisted the magnetic rotor at up to 70,200 rpm after a 65°C heat pulse was delivered.